WILEY | Hindawi

Research Article

Transport Characteristics of Tailing Sand Particles under Slotted Tube Overlapped with Geotextile and Steel Mesh

Chun-bo Yang [iD],[1] Lin-bing Wang,[2] Yuan Wang,[3,4] Qing-wen Li [iD],[3] and Jing-qi Huang [iD][3]

[1]National Center for Material Service Safety, University of Science and Technology Beijing, Beijing 100083, China
[2]School of Environmental, Civil, Agricultural, and Mechanical Engineering, College of Engineering, University of Georgia, Athens, GA 30602, USA
[3]Civil and Resource Engineering School, University of Science and Technology Beijing, Beijing 100083, China
[4]College of Water Conservancy and Hydropower Engineering, Hohai University, Nanjing 100124, China

Correspondence should be addressed to Qing-wen Li; qingwenli@ustb.edu.cn

Compared with a one-dimensional test, a two-dimensional test has the potential to study the transport characteristics of particles in tailings under different filtration materials. Due to the different test conditions and the complex test environment, the existing devices generally have limited measuring range or high accuracy. Thus, it is urgent to develop an advanced device to improve the ability of the transport characteristics of particles. In this study, a two-dimensional radial flow device is designed for analyzing the transport characteristics of particles which combine the water tank with adjustable pressure and the seepage body providing a tailing sand environment. An experimental system is built, and a seepage process is carried out to explore the transport characteristics of particles. The results indicate that when head difference remains stable, the mixture consisting of the tailing sand and water gradually transports to the vicinity of the slotted tube along the diameter direction. With an increase in head difference, the tailing sand particle size in the mixture shows a slow upward trend, which migrates in the tailing sand. And the proportion of tailing sand particles with different sizes varies under different head differences. Separation of the mixture consisting of tailing sand particles and water occurs near infiltration material, while the mixture has different transportation laws under different filtration materials. Under geotextile, most fine tailing sand particles which transport from the edge remain in geotextiles, causing an increase in the proportion of fine particles around the slotted tube. However, most fine particles pass through steel mesh, leading to a decrease in the proportion of fine particles.

1. Introduction

Particle flow composed of solid particles is very common in the process of geomechanics, such as avalanches, decomposed landslides, or debris flows. The flow characteristics of these granular materials are very different in the flow shape and evolve with time and space. The dense granular flow is often divided into three different flow patterns [1–5]: quasistatic flow, rapid dilute flow, and slow flow, as shown in Figure 1. When studying such problems, many scholars study them in multiphase flow. Li et al. [6] investigated the grain size distribution of the deposits and the corresponding segregation process of granular flows with different fractal dimensions and found that the enrichment

of the fine particles had an effect on the motion process of particles. Liu and Feng [7] developed a multiscale coupling finite element method based on the microscopic soil particle motions to investigate the influence of the physical details and kinematic characteristics of soil at the microscale associated with the global mechanical responses. Tan et al. [8] studied the effects of different densities and diameters on the speed of single particles and the time of the particle passage through the pump, and the results show that with the increase in diameter and density, the wrap angle of motion of particles increased. Ruan et al. [9] indicated that the local low permeability lens in the porous medium is caused by the pollutants blocked which will be accumulated on its surface and form a pollution pool. Gao et al. [10] studied the
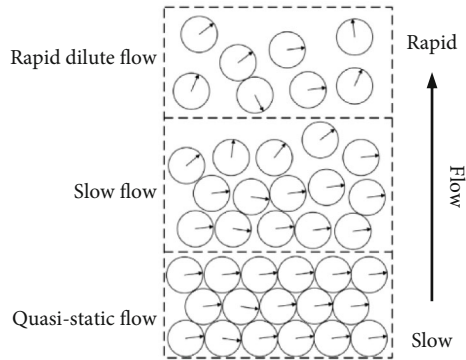
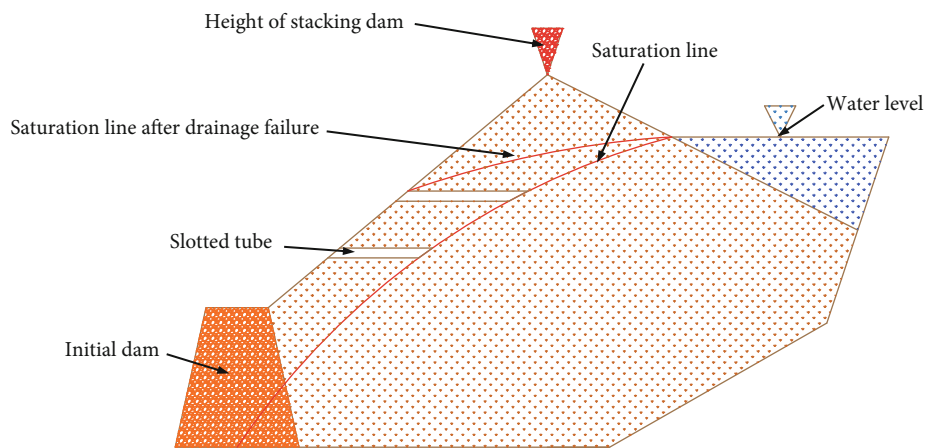Figure 1: Diagram for partition of particle flow.

Figure 2: The sketch of saturation line.

migration of dense nonaqueous-phase liquids in saturated clay based on a two-phase flow model.

As a facility for storing tailing sand, tailing ponds are formed mainly by damming valley mouths or enclosing land [11]. The transport of tailing sand particles happening in the tailing pond has a significant influence on the failure of seepage control and the high position of the infiltration line [12]. Therefore, it is of great engineering significance to carry out research on the transport process.

At present, many scholars study the clogging of filter structures caused by tailing sand, resulting in the failure of drainage facilities and the decrease of permeability coefficient. Jin et al. [13, 14] carried out a study on the drainage mechanism of the slotted tube overlay steel mesh for the fine-grained tailing dam, including the calculation method and its filter radius of the slotted tube. Yang et al. [15] investigated the effect of fine sand particles on the permeability characteristics of iron tailing sands and indicated that the permeability coefficient of iron tailing sand is affected by fine content. Mingyuan et al. [16] found that the soil desalination rate decreases with the increase in soil depth, and the distance from the pipe also affects the desalination rate through the salt discharge test. Lan et al. [17] analyzed the effect of

fine particle content on the engineering properties of tailings. Shi et al. [18] indicated that head pressure has a significant effect on particle distribution. Also, some scholars separately studied the effect of different fine particle contents on the infiltration of tailing sands and the drainage and anti-filter performance of drain pipes or geotextiles [19–23]. However, they do not detailedly study the transport process of tailing sand particles in the tailing pond, just to partly study the effect of tailing sand particles on the drainage installation.

The aim of this work was to understand the influence of filtration material applied in tailing ponds and head differences on particle transport behavior in the process of filtration and drainage. Two-dimensional radial flow tests were carried out to simulate the transfer of tailing sand particles in the solid phase. Experimental conditions (porous media, etc.) were chosen to be as close to field conditions as possible. In our study, we consider the transport process of tailing sand particles under geotextile, under steel mesh, and under different head differences. Firstly, we carry out some tests of the drainage system of the slotted tube overlay with different filtration materials including geotextile and steel mesh based on a two-dimensional radial flow test equipment. And then,
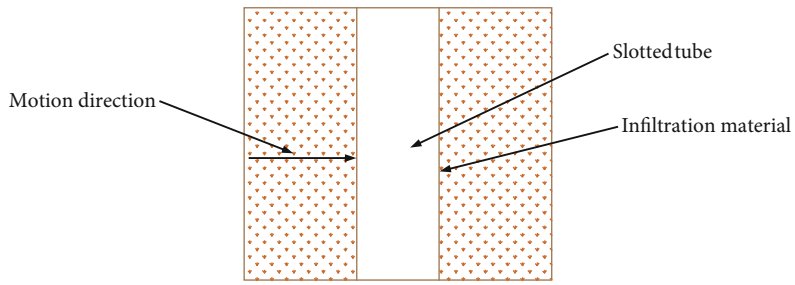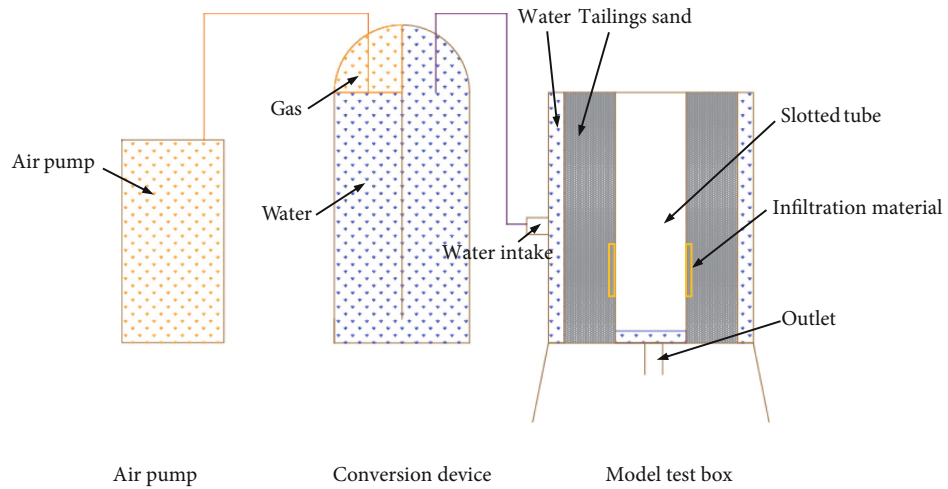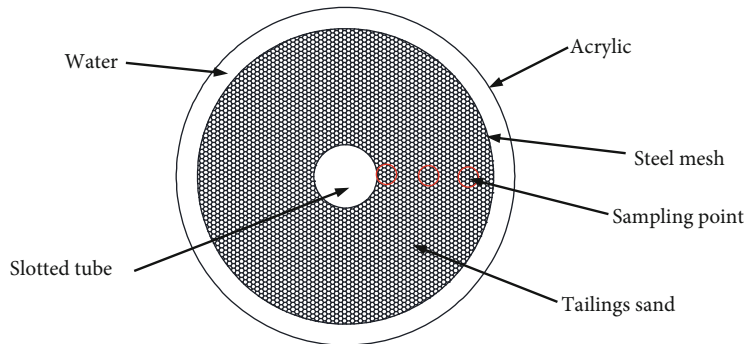
Figure 3: The motion area of tailing sand particles.

(a) Side view

(b) Top view
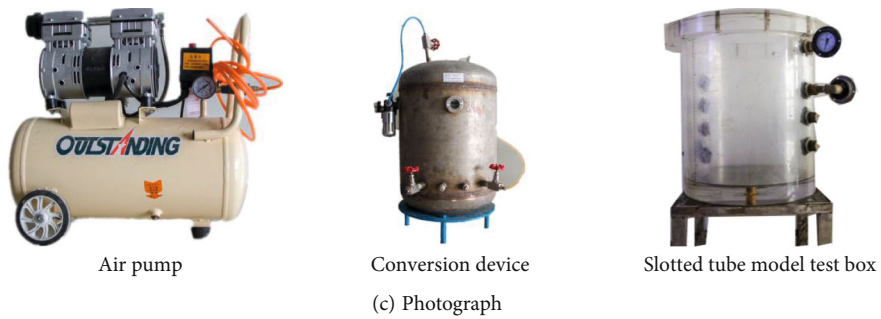
(c) Photograph

Figure 4: Experimental system and devices.

we analyze the distribution of the tailing sand particles along the diameter direction, aiming to study the effect on the transport process of tailing sand particles. The distribution of tailing sand in different positions was measured to obtain information as well as to more accurately predict the changes in the permeability of the dam body.

2. Experimental System and Test Procedure

According to the code for design of tailing facilities, the saturation line is an important lifeline of tailing ponds. Due to the clogging of drainage facilities, the saturation line changes with the permeability of filter material, as shown in Figure 2. The transport of tailing sand particles is an important reason for the decrease in drainage capacity, as shown in Figure 3. Therefore, several factors including geotextile, steel mesh, and head pressure affect the transport of tailing sand particles.

2.1. Experimental Setup. A two-dimensional pressurized radial flow experimental system was designed according to the transport characteristic of particles in the tailing dam. The system consisted of a model test box, an air pump device, and a conversion device, as shown in Figure 4, where the different parts are distinguished by different colors. Overall, this system with controlled water pressure provides multiple advantages such as simple structure, strong repeatability, and automatic operation during the entire process.

2.1.1. Model Test Box. The test box was mainly composed of an acrylic barrel, a steel mesh, a slotted tube, and a seal cover. The acrylic barrel measured $\varphi500 \times 450$ mm, and it is placed at a height of 0.25 m from the ground. A steel mesh was placed in the acrylic barrel. The slotted tube measured $\varphi100 \times 450$ mm, which was fixed in the acrylic barrel, and also, the tailing sand was filled between the steel mesh and the slotted tube. Moreover, water was filled between the steel mesh and the acrylic barrel.

2.1.2. Conversion Device. Indoor seepage experiments typically increase the pressure by the air pump. In this study, a safer and more stable conversion device was used to apply water pressure to the system to simulate pressure. The conversion device was placed on the ground beside the model test box, and the water pipeline was connected to the side face of the box. In addition, the conversion device was equipped with OPG (oil pressure gauge), as shown in Figure 5. An oil pressure gauge was used to adjust the water pressure input into the test box. Thus, the head difference could be obtained from water pressure through the calibration of OPG values. Therefore, the data on head differences could be displayed and recorded in real time during the seepage process.

2.1.3. Laser Particle Size Analyzer. A laser particle size analyzer is a commonly used equipment for analyzing particle size composition, with high accuracy, repeatability, and stability, as shown in Figure 6. After the seepage experiment, samples were taken along the diameter direction of the tailing sand permeability body. After drying and grinding, the samples were analyzed by a laser particle size analyzer to obtain the particle size composition of each sample.

2.2. Seepage Test Procedure

2.2.1. Slotted Tube Overlap Infiltration Material. The slotted tube overlap infiltration material is frequently used as the drainage equipment in the tailing pond; however, the drain-

Figure 5: The photograph of oil pressure gauge.

Figure 6: The photograph of laser particle size analyzer.

age equipment is always affected by clogging. The transport of tailing sand particles is one of the important reasons for clogging. However, there are different performances in different infiltration materials. Three groups of experiments were conducted to study the effects of different infiltration materials and head differences (see tests (a) and (b) in Table 1). Polyester geotextile was used in test (a), but steel mesh was used in test (b). According to the actual environment, the infiltration material wrapped in the slotted tube was designed to be 1.

2.2.2. Seepage Body Building. Fine tailing sand taken from the third tailing pond of the Jinchuan Concentrator at the same position of the same layer was selected as the experimental material, and its parameters are listed in Table 2. The gradation curve of the tailing sand is shown in Figure 7. In practical engineering, there are two kinds of infiltration materials including geotextile and steel mesh. Therefore, geotextile and steel mesh are adopted to study the transport characteristics of tailing sand particles in this paper. First, the mixture of tailing sand and water was stirred evenly, making the tailing sand saturated. After standing the mixture for 24 h, the interlayer between the open acrylic box was filled with layers of 450 cm saturated tailing sand, compacted to meet the density of test requirements. Besides, the strain sensor was patched outside the slotted tube and inside the steel mesh in the filling process. The shaped seepage body was $\varphi450 \times 450$ mm, as shown in Figure 8. Then, the tailing sand body was placed in the laboratory for one day, and it remained moisturized. When the tailing sand body

TABLE 1: Test details.

Test number	Slotted tube	Polyester geotextile	Steel mesh
(a)	Length: 450 mm External diameter: 100 mm Internal diameter: 80 mm	Weight: 600 g Thickness: 6.5 mm	None
(b)	Length: 450 mm External diameter: 100 mm Internal diameter: 80 mm	None	Mesh number: 100

TABLE 2: Tailing sand parameters.

(a) Particle content of each tailing sand used in the experiment

Grain group	>0.3	>0.2	>0.1	>0.085	>0.074	>0.035
Percentage	0.15	6.88	3.02	2.93	19.23	67.79

(b) Mechanical properties of the soil

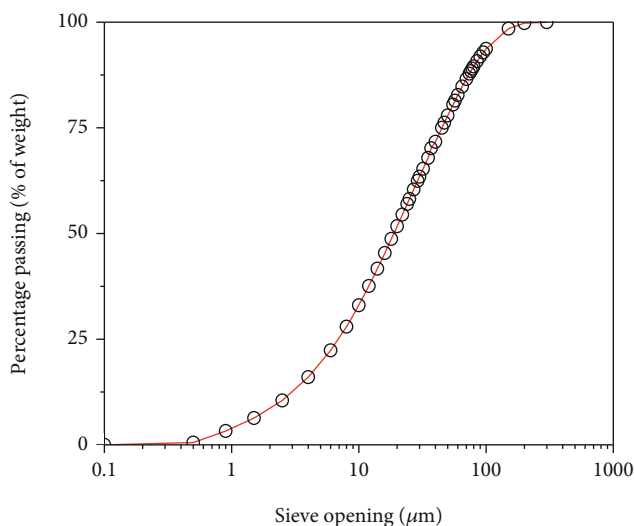|	Unevenness coefficient	Curvature coefficient	Particle density (mg·m^{-3})	Plastic limit (%)	Liquid limit (%)
Tailing sand	11.19	1.12	2.65 g/cm^3	15.49	24.74

FIGURE 7: Gradation curve of Jinchuan tailing sand.

is pushed by the water pressure, tailing sand particles move inside the tailing sand. Finally, sampling followed along the diameter direction of the seepage body after the test, and the particle size of each sample is obtained by the laser particle size analyzer.

2.2.3. Pressing Procedure. The nature head difference was used at the primary stage of the experiment. After that, the test entered the compressed stage including three substages, and the entire process simulation of a seepage test was completed in a relatively long time. Under the control of the oil pressure gauge, the water pressure could keep stable; thus, the compressed process was stable, and a smooth velocity-time curve could be obtained. The three experiments used the same tailing sand and repeated the same process of the seepage procedure. The designed two-stage process included a primary stage of 225 min. This was followed by a compressed stage of 540 min. After that, keep the head difference in the third substage and then sample at intervals to study

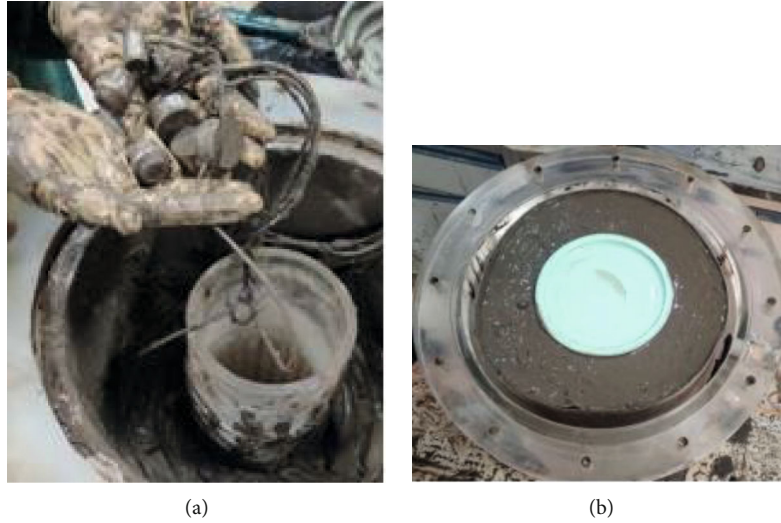(a)   (b)

FIGURE 8: (a) The photograph of strain sensor; (b) the photograph of seepage body.

TABLE 3: Volume fraction of tailing sand under different head differences.

(a)

Particle size (μm) Volume fraction	1	2	3	4	5	6	7	8	9
Original sample (%)	2.9	6.3	9.1	11.7	13.9	16.0	17.9	19.6	21.2
First substage (%)	3.4	7.1	10.2	13.1	15.6	17.9	20.0	22.0	23.6
Second substage (%)	3.4	7.2	10.5	13.4	16.0	18.4	20.5	22.4	24.2
Third substage (%)	3.1	6.7	9.6	12.3	14.7	16.9	18.9	20.8	22.5

Note: the compressed stage is divided into the first substage, second substage, and third substage.

(b)

Particle size (μm) Volume fraction	10	20	30	40	50	60	70	74
Original sample (%)	22.7	34.2	42.4	49.5	56.0	61.8	67.1	69.1
First substage (%)	25.3	37.4	46	53.4	60.0	65.8	70.9	72.8
Second substage (%)	25.8	37.5	45.8	52.9	59.4	65.2	70.3	72.2
Third substage (%)	24.1	36.2	45.1	52.8	59.6	65.7	71.1	73.0

the effect of different infiltration materials on the transport of tailing sand particles.

3. Results and Analysis

The blocking state determines the saturation line. Further, the transport process of tailing sand particles can accurately describe the change of clogging of infiltration materials. Thus, clarifying the relationship among head difference, infiltration materials, and transport process of particles can be helpful to understand the law of clogging evolution.

3.1. Head Difference and the Transport Process of Particles.
The volume fraction of particle size is calculated by the laser particle size analyzer at different sampling points, which are listed in Table 3 (0.074 mm chosen as the upper limit is the main basis for the classification of tailing sand). From the table, it can be found that head difference affects the transport process of tailing sand particles, which are analyzed in detail in the subsection.

Figure 9 shows the relationship between the head difference and the volume fraction of the tailing sand particles. The curve obtained by the tests shows increasing characteristics with the head difference increasing compared with the original sample. However, there are different phenomena under different substages. In detail, the first substage and second substage have a great influence on particle transport of 1 μm-10 μm tailing sand, while particles above 10 μm play a dominant role under the third substage. And fine particles begin to move first during the transport process. It is worth
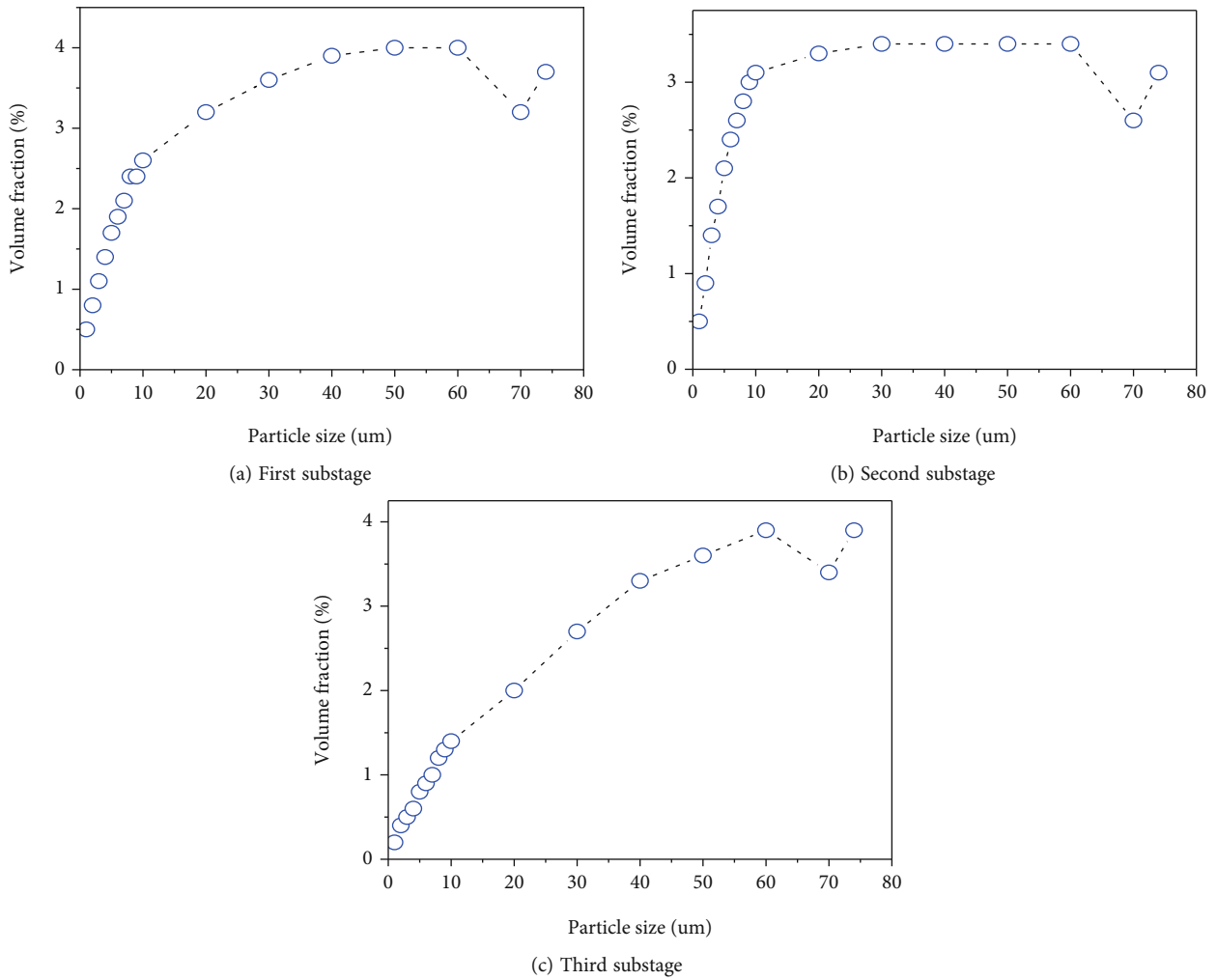
(a) First substage

(b) Second substage

(c) Third substage

FIGURE 9: Comparison of particle size with the original sample under different head differences.

(a) Volume fraction at first substage compared with that at second substage

(b) Volume fraction at second substage compared with that at third substage

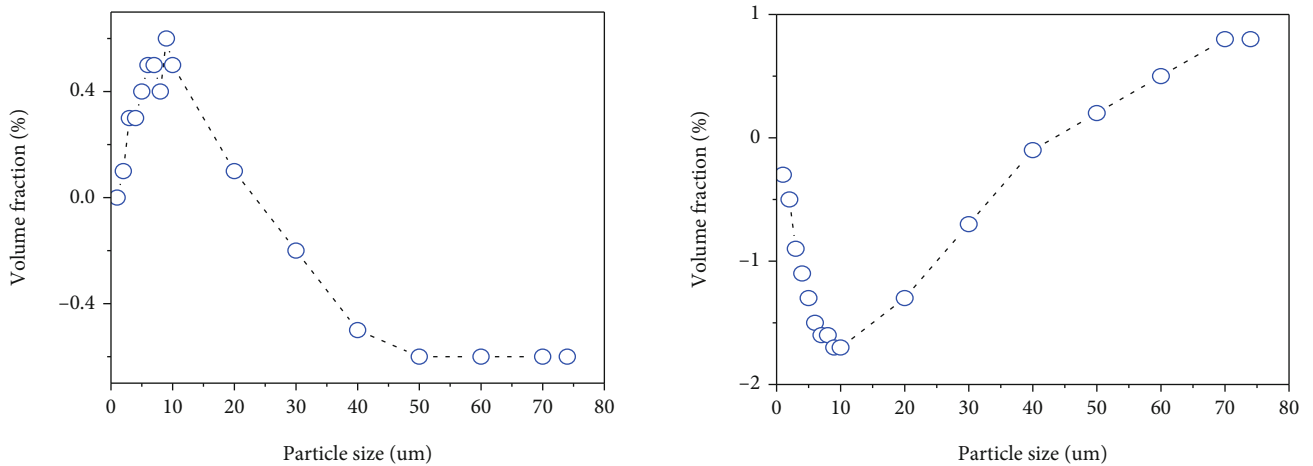FIGURE 10: Effect of different head differences on the transport of particles.

mentioning an interesting behavior that particles below $10\,\mu m$ accounted for 70.3% under the first substage. Under the second substage, particles below $10\,\mu m$ occupied the entire part, and the rate is as high as 100%. But the proportion of particles below $10\,\mu m$ is 35.9% under the third substage. Another interesting feature, compared with the first

(a) Pretest tailings sand area
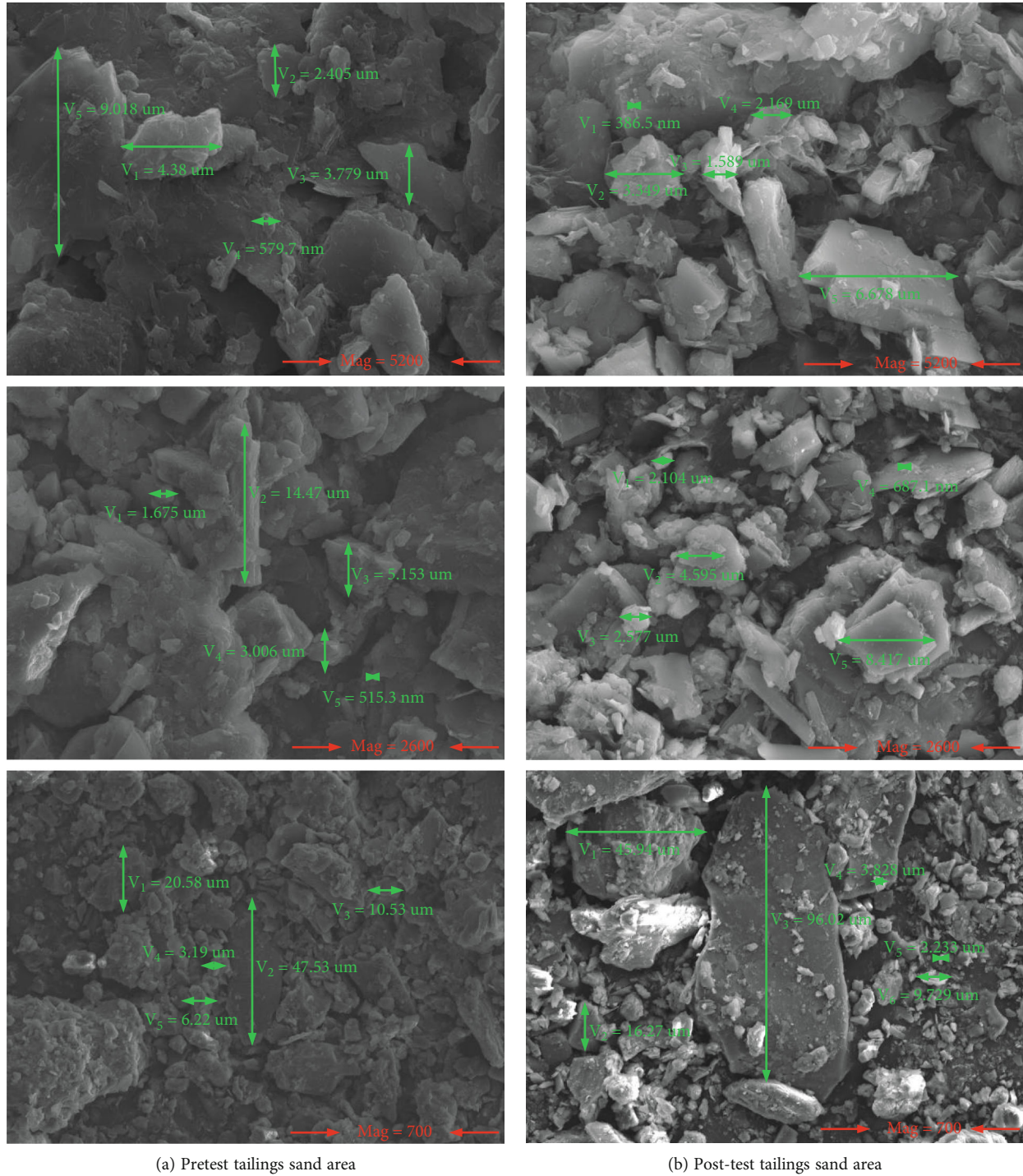
(b) Post-test tailings sand area

FIGURE 11: Scanning electron microscopy of tailing sand particles in different areas (Mag is the abbreviation of magnification).

substage, is that there is a high percentage of volume of particles below 20 μm under the second substage, especially particles below 10 μm, which indicates that the second substage has a great effect on the transport process of particles below 10 μm, as shown in Figure 10(a). In comparison with the second substage, the third substage has a great effect on particle transport of 40 μm-70 μm tailing sand, as shown in Figure 10(b). Therefore, it can be found that particle size

TABLE 4: The direct shear test results of tailing sand.

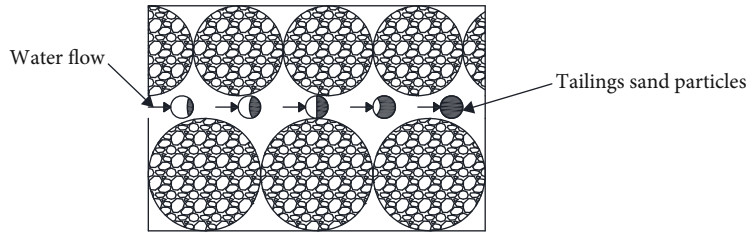| Types	Cohesion (c) (kPa)	Internal friction angle (φ) (°)
Sand	0	15
Tailing sand	8.8	27.8
Clay	12	20

FIGURE 12: Diagram of tailing sand particle motion process.

TABLE 5: Volume fraction of tailing sand under geotextile.

(a)

Particle size (μm) Volume fraction	1	2	3	4	5	6	7	8	9
Original sample (%)	2.9	6.3	9.1	11.7	13.9	16.0	17.9	19.6	21.2
First time (%)	3.1	6.7	9.6	12.3	14.7	16.9	18.9	20.8	22.5
Second time (%)	3.18	6.84	9.84	12.6	15.04	17.28	19.34	21.26	22.98
Third time (%)	3.23	6.9	9.92	12.69	15.14	17.39	19.48	21.4	23.13
Residue in geotextile (%)	3.23	9.92	9.99	12.88	15.36	17.72	19.85	21.74	23.54

Note: the compressed stage is divided into first substage, second substage, and third substage.

(b)

Particle size (μm) Volume fraction	10	20	30	40	50	60	70	74
Original sample (%)	22.7	34.2	42.4	56.0	61.8	67.1	69.1	69.1
First time (%)	24.1	36.2	45.1	59.6	65.7	71.1	73.0	73
Second time (%)	24.6	36.84	45.84	53.56	60.42	66.5	73.74	73.74
Third time (%)	24.76	37.03	46.06	53.77	60.65	66.73	73.97	73.97
Residue in geotextile (%)	25.24	39.07	49.41	57.74	64.63	70.21	76.67	76.67

TABLE 6: Volume fraction of tailing sand under steel mesh.

(a)

Particle size (μm) Volume fraction	1	2	3	4	5	6	7	8	9
Original sample (%)	2.9	6.3	9.1	11.7	13.9	16.0	17.9	19.6	21.2
First time (%)	3.39	7.02	10.1	12.86	15.35	17.59	19.63	21.51	23.24
Second time (%)	3.33	6.92	9.94	12.67	15.13	17.35	19.34	21.21	22.93
Third time (%)	3.32	6.92	9.94	12.66	15.13	17.34	19.34	21.21	22.92
Pass through steel mesh (%)	3.47	7.31	10.5	13.73	16.48	19.25	21.74	24.01	26.17

Note: the compressed stage is divided into first substage, second substage, and third substage.

(b)

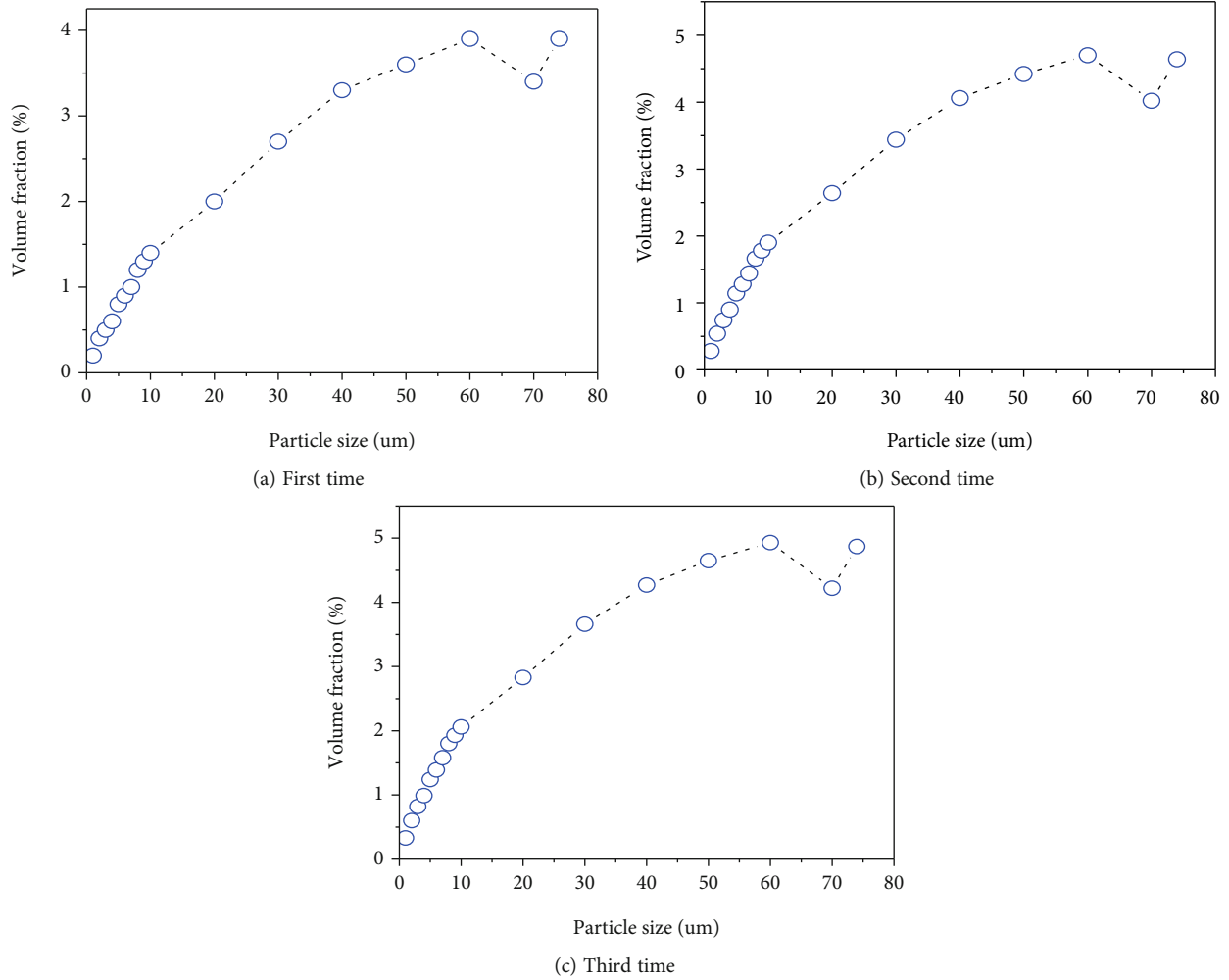| Particle size (μm) Volume fraction	10	20	30	40	50	60	70	74
Original sample (%)	22.7	34.2	42.4	49.5	56.0	61.8	67.1	69.1
First time (%)	24.85	36.71	45.01	52.11	58.5	64.2	69.22	71.04
Second time (%)	24.52	36.3	44.53	51.63	57.98	63.69	68.81	70.55
Third time (%)	24.52	36.29	44.52	51.62	57.97	63.68	68.81	70.54
Pass through steel mesh (%)	28.23	44.67	55.76	63.85	70.09	74.88	79.51	80.24

(a) First time

(b) Second time

(c) Third time

FIGURE 13: Volume fraction at different intervals compared with original sample under geotextile.

transporting to the vicinity of the slotted tube shows a stably upward trend with an increasing head difference.

As mentioned above, the head difference has a significant influence on the migration of tailing sand particles [24]. Meanwhile, it can be found from Figure 11 that there are more fine particles in the same area around the slotted tube after the test. Consequently, the results of scanning electron microscopy and grain size analysis both show that tailing sand particle transport is affected by water head difference. The reason for the phenomena is that the properties of tailing sand lie between clay and sand, which is not close between particles, as shown in Table 4 and as shown in Figure 11. The cohesion force (c) keeps at a low level, leading to a loose internal structure [25]. It indicates that seepage force easily affect tailing sand particles, causing fine particles to separate from clusters. Based on this, tailing sand particles migrate all the way towards the center of the equipment with water flow, moving in a mixture of tailing sand particles and water. Therefore, as head difference approaches the first substage, a mixture of tailing sand particles and water transports from the edge white steel mesh to the surrounding areas of the slotted tube along the diameter direction, as shown in

Figure 12. The greater the seepage force, the greater the influence of the soil particles [26]. With an increase in the head difference, coarse particles also drop from clusters, which makes it totally different from the initial water head difference. There are coarser particles in the mixture, causing a decrease in coarse particle content around the slotted tube. Based on the test data in this study, the first substage has more effect on the transport of fine particles, while the third substage has more effect on the transport of coarse particles.

3.2. Geotextile/Steel Mesh and the Transport Process of Particles. The test data about the relationship among geotextile, steel mesh, and the transport process of particles is obtained by two experiments, which are listed in Tables 5 and 6. After data processing, it is found that geotextile and steel mesh are closely related to the transport process of particles. In the subsection, the effects of geotextile and steel mesh are analyzed in detail.

3.2.1. Geotextile and the Transport Process of Particles. The figure shows the distribution of tailing sand in the transport process. The measurement results of the first time, second
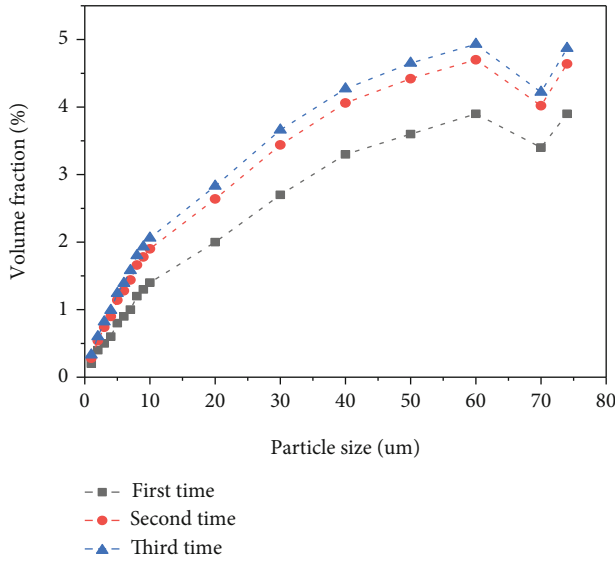
FIGURE 14: Variation of volume fraction under different intervals compared with original sample under geotextile.
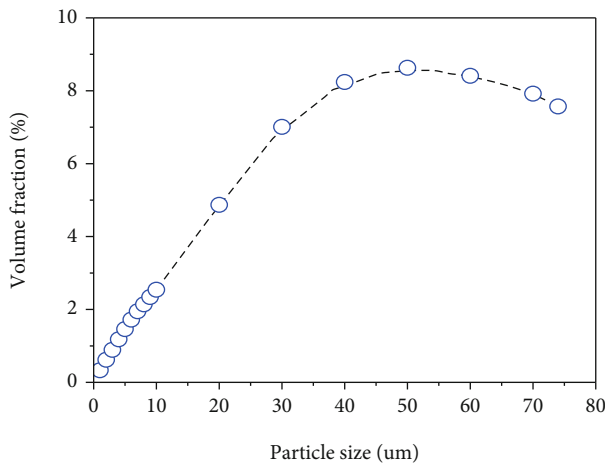

FIGURE 15: Volume fraction of tailing sand particle residue in geotextile compared with original sample.

FIGURE 16: Volume fraction of tailing sand particle residue in geotextile compared with the measurement results of the third time.

time, and third time are displayed in Figure 13. The results in Figure 14 show the variation of volume fraction under different intervals. Also, Figures 15 and 16 show tailing sand particle residue in geotextile compared with the original sample and the measurement results of the third time. It can be observed from Figure 13 that the volume fraction of fine particles around the slotted tube increases. Figure 14 illustrates that the content of fine particles increases with time when keeping the head difference stable, and the changing range is small along with the time extension. There are more tailing sand particle residues in geotextile compared with the original sample and the measurement results of the third time, as shown in Figures 15 and 16.

The phenomena are explained through the following analysis. For the phenomenon in Figure 13, there are more fine particles around the 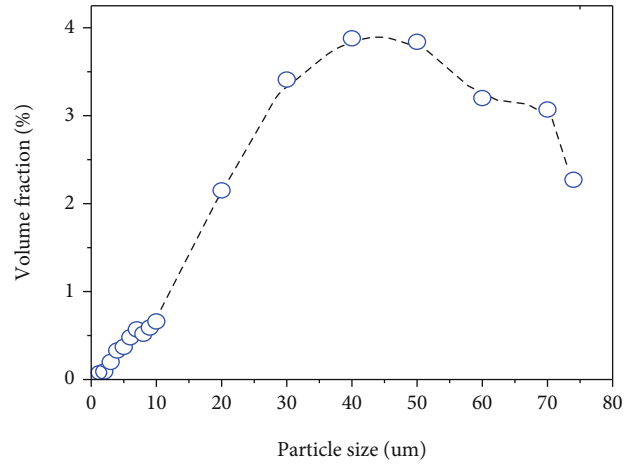slotted tube because of the seepage force, which has been made a detailed analysis in the previous section. Since head difference remains stable, the seepage force also remains constant [27], which keeps fine particles moving towards the vicinity of the slotted tube. Hence, the fine particle content is higher than the initial stage at different time points, as shown in Figure 13. However, there are different performances at different times. To know the cause of the phenomenon in Figure 14, the reason for the phenomena is first analyzed in Figures 15 and 16. Due to the filter layer formed by coarse particles around the slotted tube, fine particles with water flow pass through the filter layer in the form of a mixture under the action of seepage force [28]. The equivalent diameter of geotextile is 0.08 mm, while the particle size above 0.085 mm accounts for 2.93%, as shown in Table 2(a). Therefore, the pore size parameters of geotextile selected in the test do not match the particle gradation of tailing sand [29]. By the way, geotextile separates the mixture consisting of tailing sand and water [30]. One of the mixture, water, passes through geotextile; the other is left in geotextile, as shown in Figure 17(a). Consequently, the content of fine particles in geotextile is higher than that in the original sample, as shown in Figure 15. More fine particles in geotextile result in aggregating around the slotted tube because of limited space in geotextile which cannot accommodate more tailing sand [31]. Therefore, the proportion of fine particles increases in subsequent measurements. Based on the results, the content of fine particles in the filter layer increases with time, leading to a decrease in the seepage channel. There are less tailing sand particles entering the filter layer in unit time under the same seepage force, causing a decrease in the changing range, as shown in Figure 14. Also, the seepage channel which has decreased in the filter layer only allows finer particles to pass through. Increasing fine particle content in the geotextile is induced by the finer particles staying in the geotextile. Accordingly, fine particles occupied more and more percentage in geotextile compared with the measurement results of the third time, as shown in Figure 16.
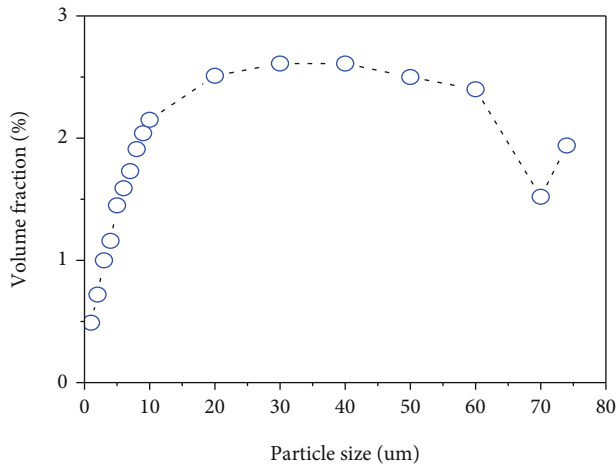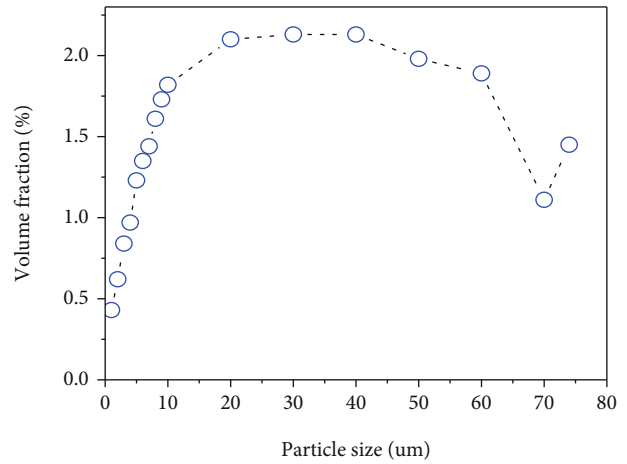
(a) Tailing sand residue in geotextile

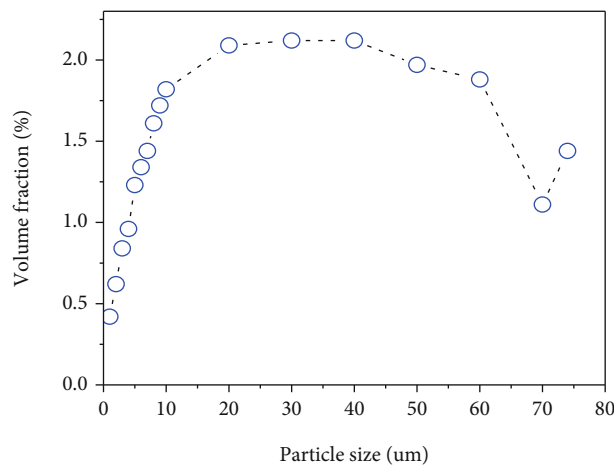(b) Water passes through the geotextile

FIGURE 17: The mixture separates into tailing sand and clear water.

(a) First time

(b) Second time

(c) Third time

FIGURE 18: Volume fraction at different intervals compared with original sample under steel mesh.
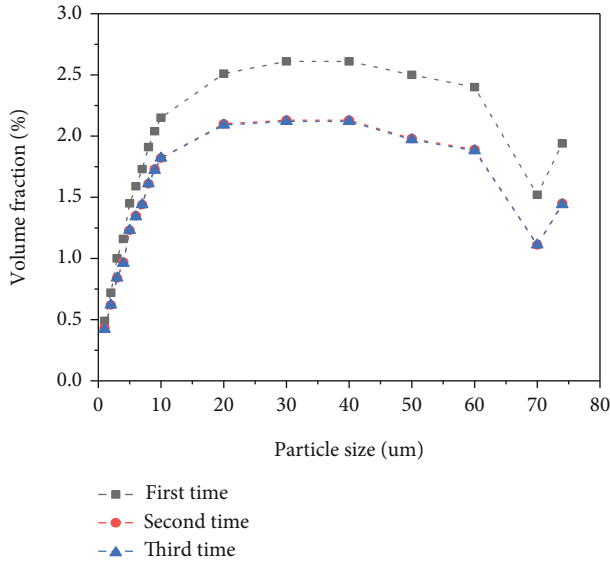
FIGURE 19: Variation of volume fraction under different intervals compared with original sample under steel mesh.

In accordance with the analysis above, we can know the transport process of the mixture consisting of tailing sand and water under geotextile. First, loose particles in the tailing sand structure fall off because of the effect of seepage force formed by water flow. A mixture of tailing sand particles and water migrates towards the center along the diameter direction. When arriving near the slotted tube, part of the tailing sand particles which are almost coarse particles remain to form the filter layer, and another continue to migrate in the form of a mixture. The mixture in geotextile is again separated into tailing sand particles and water. While tailing sand particles stay in geotextile, water passes through the geotextile, as shown in Figure 17. The whole transport process under geotextile is described. Besides, when the space in filtration is limited just like in geotextile, the proportion of fine particles in the filter layer increases with time, and part of the fine particles stay in filtration.

3.2.2. Steel Mesh and the Transport Process of Particles. Figure 18 shows the particle size distribution of tailing sand around the slotted tube compared with the original sample, while Figure 19 indicates the variation of volume fraction under different intervals compared with the original sample under steel mesh. And also, Figures 20 and 21 show tailing sand particles passing through steel mesh compared with the original sample and third time. The above pictures describe the variation of tailing sand on both sides of steel mesh in the transport process. As can be observed from Figure 18, it is the same as the geotextile in that the volume fraction of fine particles around the slotted tube rises when keeping the head difference stable. Figure 19 illustrates that the content of fine particles shows a smoothly downward trend to hit the lowest point with time. The volume fraction of tailing sand particles passing through steel mesh is higher than that of the original sample and third time, as shown in Figures 20 and 21.
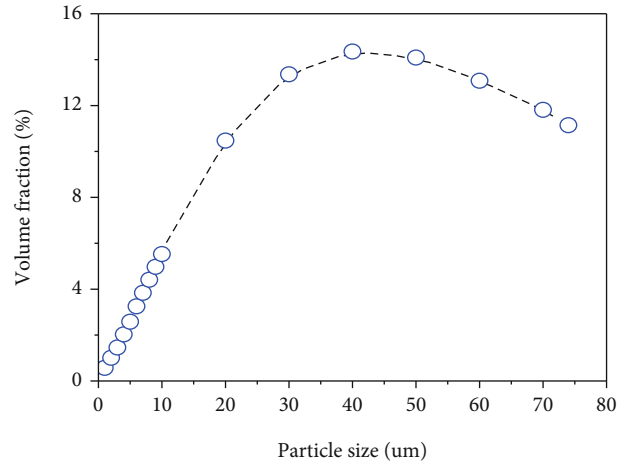

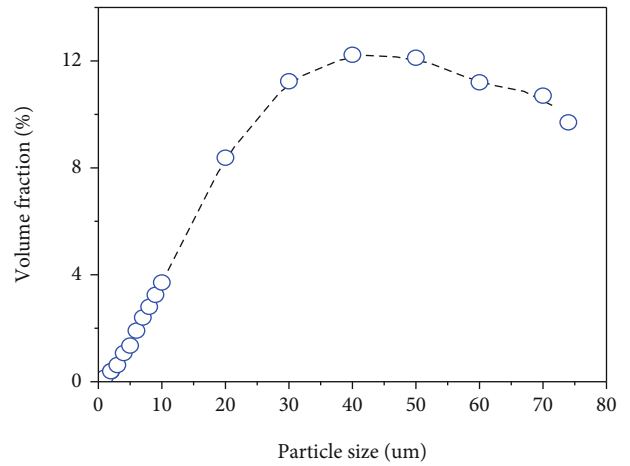FIGURE 20: Tailing sand particles pass through steel mesh compared with original sample.

FIGURE 21: Tailing sand particles pass through steel mesh compared with third time.

The reason for these phenomena can be explained as follows. For the phenomenon in Figure 18, this result is in good agreement with the previous analysis. The seepage force remaining constant makes fine particle transport to the vicinity of the slotted tube continuous. Due to the seepage force, fine particles have a higher proportion, as shown in Figure 18. When the mixture of tailing sands and water reaches the periphery of steel mesh, some fine particles with water flow pass through steel mesh, as shown in Figure 22. So, the percentage of fine particles is higher compared with the original sample, as shown in Figure 20. For the above reason, a large number of fine particles do not aggregate in the filter layer formed by the coarse particles. On the contrary, there are fewer fine particles around the slotted tube compared with the first time when measuring after a period of time. The content of fine particles in the second time and third time is almost the same. The reason for these phenomena is that the distant tailing sand particles which are in the form of a mixture pass through the filter layer when they

(a) Steel mesh after testing   (b) Water passes through steel mesh
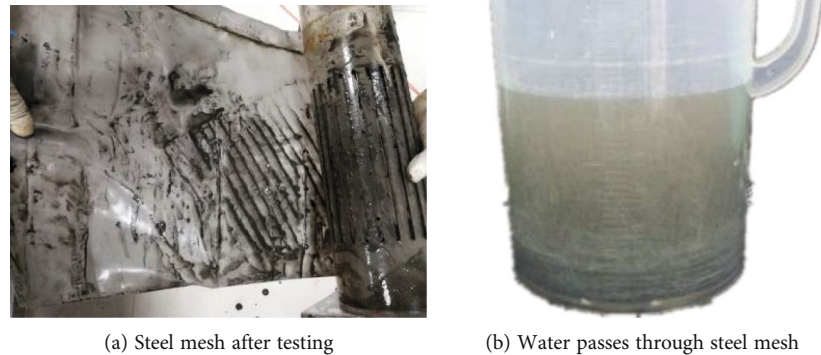
FIGURE 22: The mixture reaches the periphery of steel mesh.

reach the vicinity of the filter layer and then pass through steel mesh. Because of the phenomenon in which fine particles do not reside in the filter layer, the proportion of fine particles remain stable under the same head difference when seepage velocity keeps unchanged, as shown in Figure 19. And also for this reason, there are more fine particles in the mixture passing through steel mesh, as shown in Figure 21.

Likewise, the above shows the transport process of the mixture consisting of tailing sand and water under steel mesh. Firstly, loose particles fall from cluster transport to the vicinity of the slotted tube with water flow and gradually form a filter layer because of the effect of seepage force. However, coarse particles and fine particles have two opposite manifestations. Coarse particles are left in the filter layer, and fine particles continue to pass through steel mesh in the form of a mixture. This is the whole transport process under steel mesh. Nevertheless, when the space in filtration is not limited like steel mesh, the proportion of fine particles in the filter layer shows a steady downward trend to hit the lowest point with time, and a part of tailing sand passes through the filtration.

4. Summary and Conclusions

This study investigated the transport process of particles in the tailing sand through water pressure control. A model test of two-dimensional radial flow was designed, and one pressure was used to simulate the typical two-stage seepage process. The transport process of particles was under different head differences, geotextile, and steel mesh obtained through three comparative experiments. Then, the variation patterns of these parameters and their relationship were analyzed. Owing to the difference between the size, boundary conditions, and tailing sand properties of the experimental seepage body and actual geological conditions, an integrated discriminant criterion based on head difference, infiltration material, and transport process of particles may be applied

to practical engineering only after further verification. The primary conclusions of this study are as follows:

(1) Head difference has a relative influence on the transport process of the mixture. When the type of filtration is constant, tailing sand particle transport to the vicinity of the slotted tube due to the effect of seepage force. The proportion of tailing sand particles is different under different head differences during the transport process. The percentage of coarse particles increases during the transport processes with an increasing head difference

(2) When keeping the head difference stable, the transport process of particles changes with the variation of filtration. The content of fine particles passing through steel mesh is higher than that passing through geotextile. Under geotextile, the mixture consisting of tailing sand and water separates in the geotextile. Part of tailing sands are left in the geotextile, and another pass through the geotextile. The tailing sand particles staying in geotextile cause the proportion of fine particles around the slotted tube increasing with time. Under steel mesh, the mixture passes through steel mesh and filter layer formed by coarse particles, leading to the proportion of fine particles around the slotted tube showing a steady downward trend to hit the lowest point with time

Data Availability

The data that support the findings of this study are openly available.

Conflicts of Interest

The authors declare that they have no conflicts of interest.

Acknowledgments

References

[1] Q. Sun and G. Wang, *Introduction to Granular Material Mechanics*, Science Press, 2009.

[2] Y. Forterre and O. Pouliquen, "Flows of dense granular media," *Annual Review of Fluid Mechanics*, vol. 40, no. 1, pp. 1–24, 2008.

[3] P. Chaksmithanont, F. Milman, C. Leung et al., "Scale-up of granular material flow in an agitated filter dryer," *Powder Technology*, vol. 407, article 117684, 2022.

[4] L. Deng, H. Yuan, J. Chen et al., "Experimental investigation on progressive deformation of soil slope using acoustic emission monitoring," *Engineering Geology*, vol. 261, article 105295, 2019.

[5] G. G. Zhou and Q. C. Sun, "Three-dimensional numerical study on flow regimes of dry granular flows by DEM," *Powder Technology*, vol. 239, pp. 115–127, 2013.

[6] K. Li, Y. Wang, Q. Cheng, and X. Lin, "Effects of fractal particle size distribution on segregation of granular flows," *Chinese Journal of Rock Mechanics and Engineering*, vol. 40, no. 2, pp. 330–343, 2021.

[7] J. Liu and D. Feng, "A multi-scale coupling finite element method based on the microscopic soil particle motions," *Rock and Soil Mechanics*, vol. 42, no. 4, pp. 1186–1200, 2021.

[8] M. Tan, X. Wang, X. Wu, H. Liu, and Y. Lian, "Single particle motion visualization test of solid-liquid two-phase flow in a double-blade pump," *Journal of Harbin Engineering University*, vol. 41, no. 5, pp. 676–683, 2020.

[9] D. Ruan, J. Bian, Q. Wang, J. Wu, Y. Wang, and X. Sun, "The migration and transformation of light non-aqueous fluid in silty clay," *China Environmental Science*, vol. 41, no. 4, pp. 1815–1823, 2021.

[10] Y. Gao, S. Zhang, T. Li, and C. Shen, "Numerical analysis of vertical migration of dense nonaqueous-phase liquids in saturated clay," *Journal of Tongji University*, vol. 48, no. 1, pp. 24–32, 2020.

[11] A. Liu and A. Liang, "Comprehensive application of geosynthetics in solidified soil sea dike projects," *Chinese Journal of Geotechnical Engineering*, vol. 38, no. S1, pp. 177–180, 2016.

[12] Y. Tao, S. Wang, and D. Xu, "Experimental study of clogging defense measures for improved subsurface drainage," *Transactions of the Chinese Society for Agricultural Machinery*, vol. 47, no. 6, pp. 187–192, 2016.

[13] S. Jin, H. Xu, W. Zhang, H. Yan, and Z. Wu, "Research on calculation method and drainage mechanism of slotted pipe in fine-grained tailings dam," *Metal Mine*, vol. 441, no. 3, pp. 42–44+48, 2013.

[14] S. L. Jin, *Application Study of Slotted Orifice Pipe in Fine-Grained Tailings Dam Controlled Infiltration Line*, North China University of Technology, 2013.

[15] X. Yang, Y. Zhang, D. Gan, and Y. Jia, "Experimental study on permeability characteristics of undisturbed iron tailings," *Advanced Engineering Sciences*, vol. 52, no. 1, pp. 110–117, 2020.

[16] C. Mingyuan, H. Jiesheng, Z. Wenzhi, A. Chang, L. Dan, and L. Yi, "Characteristics of water and salt transport in subsurface pipes with geotextiles under salt discharge conditions," *Transactions of the Chinese Society of Agricultural Engineering (Transactions of the CSAE)*, vol. 36, no. 2, pp. 130–139, 2020.

[17] Q. Lan, Q. Chun-lai, and C. Ming, "Effect of fines content on engineering characteristics of tailings," *Rock and Soil Mechanics*, vol. 36, no. 4, pp. 923–927+945, 2015.

[18] Y. Shi, C. Li, and D. Long, "Meso-structure features of fine tailings sand in osmotic destruction," *Journal of Xian Jiao Tong University*, vol. 54, no. 4, pp. 155–164, 2020.

[19] G. Yin, X. Jing, Z. Wei, and X. Li, "Study of model test of seepage characteristics and field measurement of coarse and fine tailings dam," *Chinese Journal of Rock Mechanics and Engineering*, vol. 29, no. S2, pp. 3710–3718, 2010.

[20] J. Pan, Y. Wang, Y. Song, H. Jiang, G. Lei, and M. Yang, "Effect of fines content on undrained shear strength of tailings under high stress," *Metals and Minerals*, vol. 44, no. 9, pp. 166–169, 2015.

[21] S. Liu, Y. Wang, and D. Feng, "Experimental study on drainage characteristics of new composite drainage pipes in tailings pond," *Chinese Journal of Geotechnical Engineering*, vol. 41, no. 12, pp. 2360–2366, 2019.

[22] J. Chen and X. Liu, "Influence of different drainage pipe arrangement schemes on the seepage line of seepage field in tailings reservoi," *Light Metals*, vol. 29, no. 18, pp. 109–116, 2013.

[23] S. Zhang, T. Bao, C. Yoo, C. Liu, and P. Li, "Design, test and engineering application of a composite waterproof and drainage system in tunnels," *China Journal of Highway and Transport*, vol. 34, no. 4, pp. 198–208, 2021.

[24] Y. Liang, Y. Zhou, P. Lyu, and X. Shi, "Experimental study on fine particle migration in filter layer system affected by particle gradation," *Water Resources and Hydropower Engineering*, vol. 51, no. 4, pp. 152–158, 2020.

[25] S. Wu, C. Yang, X. Hu, and X. Jing, "Research on correlation of tailings particle properties and compression consolidation properties," *Journal of Huazhong University of Science and Technology (Natural Science Edition)*, vol. 45, no. 11, pp. 121–126, 2017.

[26] L. Chen, W. Lei, H. Zhang, J. Zhao, and J. Li, "Laboratory simulation and theoretical analysis of piping mechanism under unsteady flows," *Chinese Journal of Geotechnical Engineering*, vol. 35, no. 4, pp. 655–662, 2013.

[27] L. Chen, Y. Zhuang, Q. Xu, and Z. Wang, "Test study on filtration mechanism of siltnet system under limit soil-retained state," *Rock and Soil Mechanics*, vol. 29, no. 6, pp. 1455–1460, 2008.

[28] Y. Liu, D. Zheng, B. Yang, B. Zhu, and M. Sun, "Microscopic simulation of influence of particle size and gradation on permeability coefficient of soil," *Rock and Soil Mechanics*, vol. 40, no. 1, pp. 403–412, 2019.

[29] State Textile Industry Bureau of People's Republic China, *Specification for Geotextiles (GBT 17638-2008)*, China Planning Press, Beijing, 2008.

[30] A. Markiewicz, M. Kiraga, and E. Koda, "Influence of physical clogging on filtration performance of soil-geotextile interaction," *Geosynthetics International*, vol. 29, no. 4, pp. 356–368, 2022.

[31] P. Wang, Y. Han, Y. Zhou et al., "Apparent clogging effect in vacuum-induced consolidation of dredged soil with prefabricated vertical drains," *Geotextiles and Geomembranes*, vol. 48, no. 4, pp. 524–531, 2020.